

# The Post-Common Envelope and Pre-Cataclysmic Binary PG 1224+309<sup>1</sup>

Jerome A. Orosz<sup>2</sup>, Richard A. Wade, and Jason J. B. Harlow<sup>2</sup>

*Department of Astronomy & Astrophysics, The Pennsylvania State University, 525 Davey Laboratory, University Park, PA 16802-6305*  
*orosz@astro.psu.edu, wade@astro.psu.edu, harlow@astro.psu.edu*

John R. Thorstensen and Cynthia J. Taylor

*Department of Physics and Astronomy, 6127 Wilder Laboratory, Dartmouth College, Hanover, NH 03755-3528*  
*thorstensen@dartmouth.edu, Cynthia.J.Taylor@dartmouth.edu*  
 and

Michael Eracleous<sup>3,4</sup>

*Department of Astronomy, University of California, Berkeley, CA 94720*

## ABSTRACT

We have made extensive spectroscopic and photometric observations of PG 1224+309, a close binary containing a DA white dwarf primary and an M4+ secondary. The H $\alpha$  line is in emission due to irradiation of the M-star by the hot white dwarf and is seen to vary around the orbit. From the radial velocities of the H $\alpha$  line we derive a period of  $P = 0.258689 \pm 0.000004$  days and a semi-amplitude of  $K_{\text{H}\alpha} = 160 \pm 8 \text{ km s}^{-1}$ . We estimate a correction  $\Delta K = 21 \pm 2 \text{ km s}^{-1}$ , where  $K_{\text{M}} = K_{\text{H}\alpha} + \Delta K$ . Radial velocity variations of the white dwarf reveal a semi-amplitude of  $K_{\text{WD}} = 112 \pm 14 \text{ km s}^{-1}$ . The blue spectrum of the white dwarf is well fit by a synthetic spectrum having  $T_{\text{eff}} = 29,300 \text{ K}$  and  $\log g = 7.38$ . The white dwarf contributes 97% of the light at 4500 Å and virtually all of the light blueward of 3800 Å. No eclipses are observed. The mass inferred for the white dwarf depends on the assumed mass of the thin residual hydrogen envelope:  $0.40 \leq M_{\text{WD}} \leq 0.45 M_{\odot}$  for hydrogen envelope masses of  $0 \leq M_{\text{H}} \leq 4 \times 10^{-4} M_{\odot}$ . We argue that the mass of the white dwarf is closer to  $0.45 M_{\odot}$ , hence it appears that the white dwarf has a relatively large residual hydrogen envelope. The mass of the M-star is then  $M_{\text{M}} = 0.28 \pm 0.05 M_{\odot}$ , and the inclination is  $i = 77 \pm 7^\circ$ . We discuss briefly how PG 1224+309 may be used to constrain theories of close binary star evolution, and the past

<sup>1</sup>Based in part on observations obtained at the Michigan-Dartmouth-MIT Observatory.

<sup>2</sup>Visiting Astronomer at Kitt Peak National Observatory (KPNO), which is operated by AURA, Inc., under a cooperative agreement with the National Science Foundation.

<sup>3</sup>Hubble Fellow.

<sup>4</sup>Current address: Department of Astronomy and Astrophysics, The Pennsylvania State University, 525 Davey Lab, University Park, PA 16802, electronic mail: mce@astro.psu.edu

and future histories of PG 1224+309 itself. The star is both a “post-common envelope” star and a “pre-cataclysmic binary” star. Mass transfer by Roche-lobe overflow should commence in about  $10^{10}$  yr.

*Subject headings:* stars: binaries: close — stars: individual (PG 1224+309) — stars: variables — stars: white dwarfs

## 1. Introduction

PG 1224+309 was cataloged as a UV-excess object in the Palomar-Green (PG) survey (Green, Schmidt, & Liebert 1986). It also appears in the Tonantzintla survey as Ton 617 (Iriarte & Chavira 1957; Chavira 1958) and the Case low-dispersion northern sky survey as CBS 60 (Sanduleak & Pesch 1984). Its mean magnitude and colors are  $V = 16.164$ ,  $B - V = -0.065$ ,  $V - R = 0.038$ , and  $R - I = 0.312$  (this work). This object was studied by Ferguson, Green, & Liebert (1984) who were searching for cataclysmic variable-like stars in the PG survey. Ferguson et al. (1984) showed that PG 1224+309 was a binary, identified the hot star as a DA white dwarf with  $T_{\text{eff}} = 28,000$  K and  $\log g = 7.7 \pm 0.8$ , and classified the cool star as an M2 dwarf based on its colors. Refined values of  $T_{\text{eff}} = 29,300 \pm 1000$  K and  $\log g = 7.38 \pm 0.1$  for the white dwarf were later provided by J. W. Liebert & P. Bergeron (1997). PG1224+309 was not discussed again in the literature for thirteen years. Orosz, Wade, & Harlow (1997) looked for radial velocity variations in a number of stars that were characterized as composite spectrum binaries by Ferguson et al. (1984), and found for PG 1224+309 that the radial velocity of the M star changed by  $83 \pm 11$  km s $^{-1}$  between two observations  $\approx 0.9$  days apart. Orosz et al. (1997) also showed that PG 1224+309 has a strong and variable H $\alpha$  emission line. Photometric observations by S. Bell (private communication 1996) showed that the light varies smoothly on a timescale of hours.

All of these observations strongly suggested that PG 1224+309 is a close binary system, in which the M star is irradiated by the white dwarf. We therefore obtained additional photometric and spectroscopic data on this object, reported in this paper. Our goals were to characterize the orbit, to estimate the masses and other properties of the two stars, and to place the system in its evolutionary context. The additional data confirm that PG 1224+309 is a short-period, double-lined spectroscopic binary system with photometric and emission-line variations evidently caused by illumination of one hemisphere of the cool M star by the hot white dwarf. We present below a description of our observations and data analysis. We discuss various constraints on the component masses and the geometry of the system and end with a brief discussion of the evolutionary status of this binary star. Systems such as PG 1224+309 may illuminate difficult aspects

of common-envelope binary evolution.

## 2. Observations

### 2.1. MDM<sup>5</sup> Spectroscopic Observations

We obtained 55 exposures between 1996 December and 1998 March using either the 2.4 m Hiltner Telescope and modular spectrograph, or the 1.3 m McGraw-Hill Telescope and Mark III spectrograph. Table 1 summarizes the observations. The 2.4 m data had a spectral resolution of  $\sim 3.5$  Å FWHM, and the 1.3 m data had  $\sim 5$  Å, as determined from comparison lines. All spectra covered H $\beta$  to H $\alpha$ , and the later 2.4 m spectra (taken with the 2048  $\times$  2048 CCD) covered from 4000 to 7500 Å with considerable vignetting toward the ends. Individual exposures were 300 to 600 s at the 2.4 m telescope, and typically 900 s at the 1.3 m. All stellar spectra were bracketed in time with comparison-lamp exposures, and typical rms residuals of the wavelength solutions were  $< 0.1$  Å. Standard IRAF<sup>6</sup> *specred* tasks were used to subtract the electronic bias, divide by flat-fields, optimally extract one-dimensional spectra, subtract sky background, and rebin the spectra onto a uniform wavelength scale. We obtained spectra of hot stars and flux standards to convert our spectra to absolute flux units.

At the 2.4 m we used a narrow slit (1 arcsec), so our spectrophotometry suffers from variable, uncalibrated losses at the slit jaws; we estimate that this effect introduces a  $\sim 30$  percent uncertainty in our absolute flux levels. In addition, continuum shapes derived with the modular spectrograph sometimes suffer 10–20 per cent errors in their overall slopes, which we do not understand. We did rotate the spectrograph to align the slit with the parallactic angle whenever the zenith distance was substantial, so differential refraction is not the culprit.

### 2.2. Kitt Peak Photometric Observations

We obtained images of PG 1224+309 during the interval 1998 May 5–13 with the KPNO 0.9m telescope, which was equipped with the T2KA 2048  $\times$  2048 CCD at both the f/13.5 focus (May 5–8) and the f/7 focus

<sup>5</sup>MDM Observatory is operated by a consortium of Dartmouth College, Columbia University, the Ohio State University, and the University of Michigan.

<sup>6</sup>IRAF is distributed by the National Optical Astronomy Observatories.

TABLE 1  
LOG OF SPECTROSCOPIC OBSERVATIONS

Start <sup>a</sup>	Finish <sup>a</sup>	<i>N</i>	Setup	Detector
447.03	453.05	8	MDM 2.4+mod	Tek1024
486.89	491.96	18	MDM 1.3+MkIII	Tek1024
494.94	498.90	8	MDM 2.4+mod	Tek1024
623.66	630.66	7	MDM 2.4+mod	SiTe2048
800.06	801.06	2	MDM 2.4+mod	SiTe2048
842.04	846.98	8	MDM 2.4+mod	SiTe2048
894.90	895.98	4	MDM 2.4+mod	SiTe2048
955.83	955.91	8	Lick 3m + Kast	Reticon 1200 $\times$ 400
987.76	987.84	8	Lick 3m + Kast	Reticon 1200 $\times$ 400

<sup>a</sup>Heliocentric Julian date minus 2,450,000.

(May 9-13). Typical exposure times were 400 s for the *B* filter, 300 s for *V*, 200 s for (Kron-Cousins) *R*, and 250 s for (Kron-Cousins) *I*. The night of May 4/5 was photometric and we obtained 24 observations of 16 different standard stars from the list of Landolt (1992) in each of the *B*, *V*, *R*, and *I* filters, in addition to the nine *B*, *V*, *R*, and *I* sequences on PG 1224+309.

Standard IRAF tasks were used to subtract the electronic bias and perform flat-field corrections. We used the programs DAOPHOT IIe, ALLSTAR and DAOMASTER (Stetson 1987; Stetson, Davis, & Crabtree 1991; Stetson 1992a,b) to compute the photometric time series of PG 1224+309 and five nearby field stars. The observations of the Landolt standard stars were used to derive the transformation from DAO-MASTER instrumental magnitudes to the standard scales. The formal errors for the zeropoints of the calibrated magnitude scales are 0.018 mag for the *B* filter, 0.005 mag for the *V* filter, 0.012 mag for the *R* filter, and 0.013 mag for the *I* filter. Another indication of the quality of the photometric calibration comes from an examination of the measured comparison star magnitudes. Each comparison star had nine measures in the four different filters. There was very little scatter in these measurements: the standard deviations ranged from 0.003 to 0.030 mag.

### 2.3. Lick Spectroscopic Observations

Blue spectra of PG 1224 + 309 were obtained with the 3m Shane Telescope and Kast spectrograph (Miller & Stone 1993) at Lick Observatory on 1998 May 22 UT and again on 1998 June 23 UT. On each occasion the star was observed for approximately 2 hours during which a set of eight 15-minute exposures was obtained, covering about 1/3 of the orbital cycle. The purpose was to measure the radial velocity curve of the white dwarf from the high-order Balmer lines in its spectrum, so the observations were planned to sample a different part of the orbital cycle of the system on each run. The spectra cover the range 3200–4550 Å with a spectral resolution of 2.8 Å. They were obtained through a 2" slit using an 830 mm<sup>-1</sup> grism. The seeing varied between 1".5 and 2" over the course of the observations resulting in a variable loss of light at the slit jaws. Moreover, since the star had to be followed through a fairly high airmass, some spectra suffer from additional light losses at the shortest wavelengths because of differential atmospheric refraction, in spite of our efforts to keep the slit at the parallactic angle. A log of the observations is included in Table 1.

The spectra were reduced in a standard manner, as described earlier, although we used our own reduction software while making only limited use of the IRAF software package. In the final individual spectra, the

TABLE 2  
 $\text{H}\alpha$  RADIAL VELOCITIES

HJD <sup>a</sup>	V						
	(km s <sup>-1</sup> )						
447.998	-48	490.777	-73	624.656	57	846.017	163
451.052	125	491.953	2	624.660	47	846.025	161
451.058	120	491.964	-32	626.658	130	846.962	-113
487.032	20	497.888	86	626.662	172	846.969	-129
487.833	-112	497.894	77	630.658	-156	895.968	144
488.859	0	498.894	187	800.062	14	895.976	138
488.870	9	498.900	148	842.038	-154	...	
489.065	209	623.658	-75	845.010	173	...	
489.840	215	623.665	-97	846.010	147	...	

<sup>a</sup>Heliocentric JD of mid-integration minus 2450000.

signal-to-noise ratio at 4200 Å ranges between 15 and 25. The wavelength scale was originally derived from spectra of arc lamps obtained at the beginning of each sequence of object spectra. The wavelength scales of individual spectra were then refined by using the emission-line spectra of the night sky recorded during the same exposure to measure small *relative* offsets and rectifying them. As a result of this procedure, the *relative* velocity scales of individual spectra agree to 8 km s<sup>-1</sup> or better.

### 3. Data Analysis

#### 3.1. The Spectroscopic Period and the $\text{H}\alpha$ Emission Line Radial Velocity Curve

We used the set of spectra from MDM to determine the spectroscopic period since the time coverage for these data is by far the longest. The MDM spectra (discussed later) showed a narrow, variable  $\text{H}\alpha$  emission line superposed on a strong white dwarf spectrum of type DA (see also Orosz, Wade, & Harlow 1997). For 33 spectra with adequate signal-to-noise, we fitted this feature with a Gaussian, adjusting approximately for the sloping baseline caused by the white dwarf absorption. Table 2 gives the resulting radial velocities. A Gaussian-convolution algorithm (Schneider & Young 1980) gave similar results, but with slightly greater scatter around the best fit (below). We searched for periods by constructing a

highly oversampled grid of trial frequencies spanning 0 to 8 cycles d<sup>-1</sup>, fitting a least-squares sinusoid to the velocities at each frequency, and plotting the inverse of the fit variance as a function of frequency to form a ‘residual-gram’ (Thorstensen et al. 1996). This method works well when the modulation is sinusoidal and its amplitude exceeds the observational uncertainty. Figure 1 shows the result, which is consistent with a single frequency near 3.86 d<sup>-1</sup>; the cycle count is unambiguous. A least-squares sinusoid fit of the form

$$v(t) = \gamma_{\text{H}\alpha} + K_{\text{H}\alpha} \sin \left[ \frac{2\pi(t - T_0)}{P} \right]$$

gave

$$\begin{aligned} T_0 &= \text{HJD } 2450624.537 \pm 0.002, \\ P &= 0.258689 \pm 0.000004 \text{ d}, \\ K_{\text{H}\alpha} &= 165 \pm 9 \text{ km s}^{-1}, \\ \gamma_{\text{H}\alpha} &= 10 \pm 6 \text{ km s}^{-1}, \text{ and} \\ \sigma &= 29 \text{ km s}^{-1}, \end{aligned}$$

where  $\sigma$  is the uncertainty of a single measurement inferred from the goodness-of-fit, and the uncertainties are formal 1- $\sigma$  errors. Discarding the two worst-fitting points changed  $K$ ,  $\gamma$ , and  $\sigma$  to  $160 \pm 8$ ,  $8 \pm 5$ , and  $26 \text{ km s}^{-1}$  respectively, but did not significantly affect the ephemeris. Figure 2 (lower panel) shows all the velocities folded on the ephemeris. The sinusoid

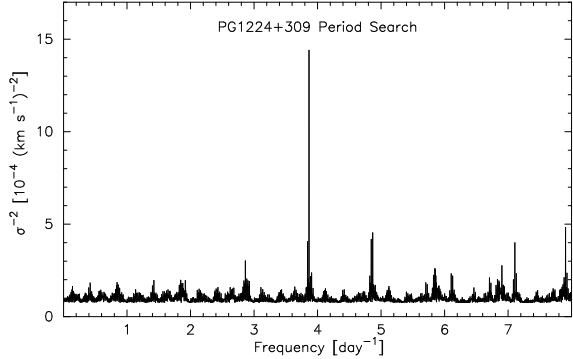


Fig. 1.— Results of a period search on the H $\alpha$  emission velocities. The vertical axis is the inverse of the variance around a sinusoidal fit at each trial frequency. In order to compress the large number of data points we show local maxima in this function, joined by straight lines.

shown has been fitted to all but the two worst points. We adopt  $K_{H\alpha} = 160 \pm 8$  km s $^{-1}$ .

The H $\alpha$  emission fits also produced estimates of the equivalent width (EW). These were noisier than the radial velocities, but showed a strong modulation at the same period. A sinusoidal fit to the EW time series, with the period fixed at the more accurately-determined radial velocity period, showed that the EW modulation lags in phase behind the radial velocities by  $0.256 \pm 0.016$  cycle. This is nicely consistent with the 0.25-cycle lag expected if the emission line arises on the side of the normal star facing the white dwarf (Thorstensen et al. 1978; Vennes & Thorstensen 1994). The upper panel of Figure 2 shows the equivalent widths folded on the best period, together with a sinusoidal fit with a half-amplitude of  $3.0 \pm 0.3$  Å and a mean of  $4.4 \pm 0.2$  Å (formal error). The sinusoidal fit is only fiducial, as the modulation may not be strictly sinusoidal (Thorstensen et al. 1978), and our EW accuracy and sampling are not sufficient for us to detect small deviations from a sinusoid. In any case, the deep modulation of the equivalent widths, and the accurate agreement of the phase offset with the illumination model, make it very likely that the bulk of the H $\alpha$  emission arises from fluorescence on the illuminated face of the normal star. It is possible that the M dwarf also has intrinsic H $\alpha$  emission, but it apparently does not dominate.

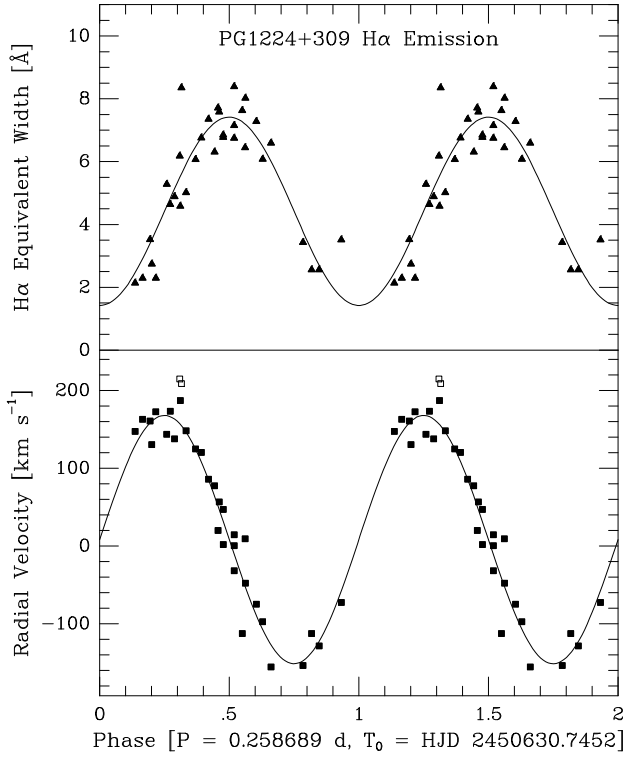


Fig. 2.— Lower panel: radial velocities of the H $\alpha$  emission lines, derived from Gaussian fits to the line profile, folded on the best period, with the best-fitting sinusoid superposed. The points represented by open squares were excluded from the fit. Upper panel: Equivalent widths of the H $\alpha$  emission line folded on the best period. The fiducial sinusoid shown is shifted by 0.25 cycle from the velocity ephemeris.

### 3.2. Photometric Variations

The  $B$ ,  $V$ ,  $R$ , and  $I$  light curves of PG 1224+304 display approximately sinusoidal modulations with a period near  $\approx 6$  hours, as expected based on the spectroscopic analysis. We fit four-parameter sinusoids to each of the four light curves (using the spectroscopic period  $P_{\text{spect}}$  as the initial period guess) to determine the photometric period, semi-amplitude, mean magnitude, and the time of photometric minimum. The results are displayed in Table 3. The errors on the individual magnitudes were scaled to give  $\chi^2_\nu = 1$  for each curve and the errors on the fitted parameters were computed from the scaled errors. The errors listed in Table 3 may have been slightly underestimated, since the light curve shapes

TABLE 3  
PHOTOMETRIC PARAMETERS

Filter	<i>N</i>	Period (days)	Semi-amplitude (mag)	Mean	$T_0$ (photo) (HJD 2450000+)	Spectroscopic phase of $T_0$ (photo)
<i>B</i>	38	$0.2587 \pm 0.0003$	$0.034 \pm 0.002$	$16.099 \pm 0.002$	$938.840 \pm 0.004$	$1214.98 \pm 0.03$
<i>V</i>	55	$0.2588 \pm 0.0001$	$0.070 \pm 0.002$	$16.164 \pm 0.001$	$938.845 \pm 0.002$	$1215.00 \pm 0.02$
<i>R</i>	39	$0.2586 \pm 0.0001$	$0.104 \pm 0.003$	$16.126 \pm 0.002$	$938.847 \pm 0.002$	$1215.01 \pm 0.02$
<i>I</i>	50	$0.2582 \pm 0.0001$	$0.098 \pm 0.002$	$15.812 \pm 0.001$	$938.849 \pm 0.001$	$1215.02 \pm 0.02$

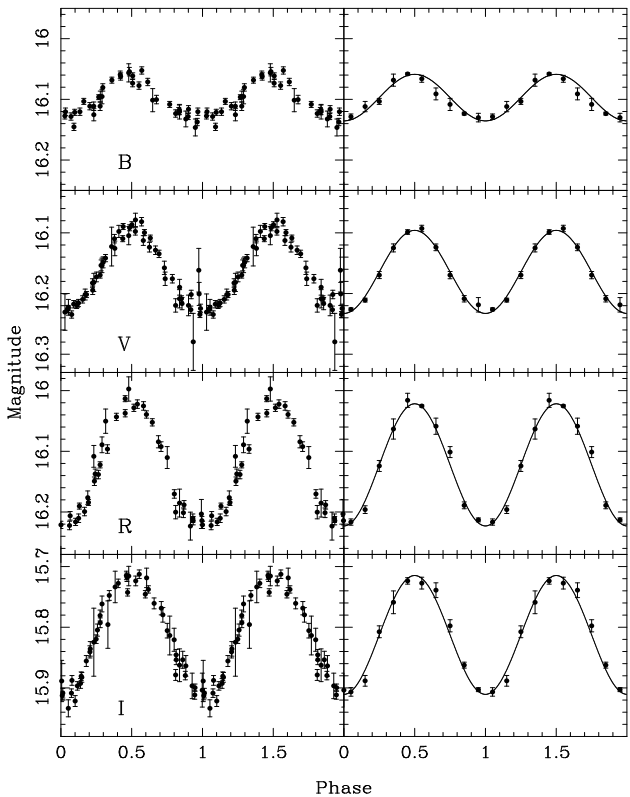


Fig. 3.— The *B*, *V*, *R*, and *I* light curves folded on the adopted (mean) ephemeris are shown in the left panels, where each point has been plotted twice. The right panels show the folded light curves binned into ten phase bins, where the error bars represent the errors of the mean in each bin. Sine curves have been added to demonstrate the absence of eclipses; the minimum of each curve occurs at phase zero, and the semiamplitudes in the *B*, *V*, *R*, and *I* bands are 0.04, 0.07, 0.10, and 0.10 mag respectively.

may not be exact sinusoids. The periods derived for the four light curves are close to the spectroscopic period. We also computed the spectroscopic phase of the time of the photometric minimum for each light curve. All of these phases are consistent with a whole number of cycles, as expected if the cause of the modulation is due to irradiation of the M star by the white dwarf. We used the weighted mean of the photometric  $T_0$  and the spectroscopic  $T_0$  (propagated forward by 1207 cycles) to define the phase zero-point for the adopted ephemeris:  $T_0$ (mean) = HJD 2, 450, 938.8430  $\pm$  0.0026. Our adopted orbital parameters are given in Table 4, and the folded light curves are displayed in Figure 3.

### 3.3. The White Dwarf Radial Velocity Curve

The radial velocity of the white dwarf was measured from each Lick spectrum by comparing it to a synthetic white dwarf spectrum, constructed with the parameters reported by Liebert & Bergeron (1997). The method involves assuming a radial velocity for the white dwarf, applying a Doppler shift and appropriate scaling to the model spectrum, and comparing it to the observed spectrum in the range 3890–4400 Å by means of the  $\chi^2$  test. By scanning a range of possible white dwarf radial velocities in very fine steps we obtain the best estimate as the one with the lowest value of  $\chi^2$  as well as error bars corresponding to 68% (1- $\sigma$ ) confidence limits. The measured heliocentric radial velocities are given in Table 5 along with their corresponding orbital phases, computed from the adopted mean ephemeris given in Table 4. In Figure 4 we plot the radial velocity of the white dwarf as a function of this orbital phase.

The observed radial velocities were fitted with a

TABLE 4  
ADOPTED ORBITAL PARAMETERS

parameters	value
$P_{\text{spect}}$ (days)	$0.258689 \pm 0.000004$
$K_{\text{H}\alpha}$ ( $\text{km s}^{-1}$ )	$160 \pm 8$
$K_{\text{WD}}$ ( $\text{km s}^{-1}$ )	$112 \pm 14$
$T_0(\text{spect})$ (HJD 2,450,000+)	$626.608 \pm 0.002$
$T_0(\text{photo})$ (HJD 2,450,000+)	$938.844 \pm 0.003$
$T_0(\text{mean})$ (HJD 2,450,000+)	$938.843 \pm 0.003$

NOTE.— $T_0$  refers to the sine-fit of radial velocities measured from the  $\text{H}\alpha$  emission line, i.e. inferior conjunction of the M star.

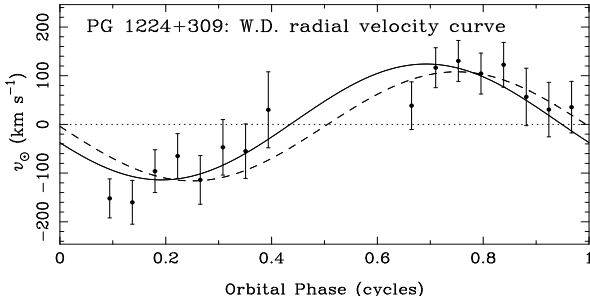


Fig. 4.— The measured radial velocity curve of the white dwarf with two circular-orbit models superposed for comparison. The radial velocities were measured from the high-order Balmer lines ( $\text{H}\gamma$ ,  $\text{H}\delta$ , and  $\text{H}\epsilon$ ) and have been corrected for the Earth's motion around the Sun. The orbital phase is computed according to the adopted (mean) ephemeris. The solid line shows a fit in which the phase of inferior conjunction of the white dwarf was treated as a free parameter, while the dashed line shows a model in which this phase was fixed at 0.5.

circular-orbit model. Because the observations do not cover a complete orbital cycle we cannot use them to obtain a measurement of the period. Hence we adopt the period derived from the  $\text{H}\alpha$  velocities and we express the model as

$$v(\phi) = \gamma_{\text{WD}} + K_{\text{WD}} \sin [2\pi(\phi - \Delta\phi)], \quad (1)$$

where  $\phi$  is the orbital phase from the adopted ephemeris ( $0 \leq \phi < 1$ ) and  $\Delta\phi$  is the phase of inferior conjunction of the white dwarf, which is expected *a priori* to be 0.5. The free parameters of the model are  $\gamma_{\text{WD}}$ ,  $K_{\text{WD}}$  and  $\Delta\phi$ . A minimum  $\chi^2$  fit of the model to the data gives the following parameters:

$$\begin{aligned} \Delta\phi &= 0.442^{+0.049}_{-0.044}, \\ K_{\text{WD}} &= 119^{+24}_{-23} \text{ km s}^{-1}, \text{ and} \\ \gamma_{\text{WD}} &= 5 \pm 21 \text{ km s}^{-1} \end{aligned}$$

with errors corresponding to 68% confidence limits. Since the best-fitting value of  $\Delta\phi$  is consistent with expectation (according to the F-test), we may fix  $\Delta\phi$  to its expected value. Under this assumption we obtain:

$$\begin{aligned} \Delta\phi &= 0.5 \text{ (fixed),} \\ K_{\text{WD}} &= 112 \pm 14 \text{ km s}^{-1}, \text{ and} \\ \gamma_{\text{WD}} &= -4 \pm 12 \text{ km s}^{-1} \end{aligned}$$

The best-fitting model radial velocity curves (with  $\Delta\phi$  both free and fixed) are superposed on the data in Figure 4, for comparison.

### 3.4. White Dwarf Atmospheric Parameters

Using the fitted radial velocity curve of the white dwarf, we corrected the Doppler shifts in the Lick spectra and averaged them together to obtain a spectrum with a high signal-to-noise ratio, which is free from orbital Doppler broadening. We chose to use

TABLE 5  
HELIOPHILIC RADIAL VELOCITIES FROM WHITE DWARF ABSORPTION LINES

HJD <sup>a</sup>	$\phi$ <sup>b</sup>	$V_{\odot}$ (km s <sup>-1</sup> )	HJD <sup>a</sup>	$\phi$ <sup>b</sup>	$V_{\odot}$ (km s <sup>-1</sup> )
955.82971	0.665	38 ± 49	987.75956	0.094	-152 ± 40
955.84151	0.710	116 ± 41	987.77064	0.137	-160 ± 45
955.85258	0.753	130 ± 42	987.78170	0.180	-96 ± 44
955.86365	0.796	104 ± 42	987.79276	0.222	-65 ± 46
955.87471	0.839	122 ± 46	987.80385	0.265	-114 ± 50
955.88578	0.881	56 ± 59	987.81493	0.308	-47 ± 57
955.89683	0.924	30 ± 56	987.82601	0.351	-55 ± 56
955.90792	0.967	35 ± 53	987.83709	0.394	30 ± 78

<sup>a</sup>Heliocentric JD of mid-integration minus 2450000.

<sup>b</sup>Orbital phase, computed from the adopted (mean) ephemeris.

four of the Lick spectra for this purpose, namely the ones spanning orbital phases 0.09 to 0.22. These four spectra were obtained under the best seeing conditions and at the lowest airmass. As a result they individually have a high signal-to-noise ratio and the effects of differential atmospheric refraction are negligible. Also, the line-emitting face of the secondary star is directed mainly away from the observer at these orbital phases. Hence the contamination of the cores of the absorption lines in the white dwarf spectrum by narrow emission lines is minimal. The average spectrum of the white dwarf is shown in Figure 5.

We used this Lick “restframe” spectrum with its improved signal-to-noise to estimate values of the white dwarf surface gravity  $\log g$  and effective temperature  $T_{\text{eff}}$ . (Recall that  $T_{\text{eff}} = 29,300$  K and  $\log g = 7.38 \pm 0.1$  according to Liebert & Bergeron [1997]. Their uncertainties include estimates of the systematic errors due to modeling assumptions and input physics.) We computed a grid of pure hydrogen, LTE model spectra, covering the range  $\log g = 7.18$  to 7.58 in steps of 0.1 and the range  $T_{\text{eff}} = 28,300$  K to 29,800 K in steps of 500 K. These synthetic spectra were computed using I. Hubeny’s programs TLUSTY and SYNSPEC, and the broadening of the hydrogen lines was treated using the tables of Schoening and Butler (see Hubeny & Lanz 1997). We fitted the Lick restframe spectrum over the wavelength in-

terval 3700–4533 Å, excluding the Ca II H and K lines and features at approximately 4018 and 4174 Å.

The observed spectrum of PG 1224+309 consists of *three* components: the white dwarf spectrum, the spectrum of the late-type secondary (see below), and the spectrum from the heated face of the secondary. It is likely that the unilluminated portion of the M star does not make a noticeable contribution in the *U* and *B* bands, but the same thing cannot be said about the heated face of the M star. The Lick restframe spectrum was constructed so that the contamination from the heated face was minimized as much as possible, but the fact that the H $\alpha$  emission line is always visible suggests that some of the heated hemisphere is visible near phase 0.0. To allow for this extra light, we used a fitting method similar to the one given in Marsh, Robinson, & Wood (1994), which can be summarized as follows. The data and models are all normalized at a common wavelength (4501 Å). Each model spectrum is scaled by an amount  $w$  ( $0 \leq w \leq 1$ ) and subtracted from the data, a third-order polynomial is fitted to the residuals, and the rms residual of the fit is recorded. The optimal fit is defined to be the one that gives the lowest overall value for the rms, corresponding to the “smoother” difference spectrum. Here we are assuming that the spectrum of the irradiated hemisphere is featureless. The best decomposition is shown in Figure 5. The model white dwarf

spectrum has  $T_{\text{eff}} = 29,300$  K and  $\log g = 7.38$  and contributes 97% of the light at 4500 Å and virtually all of the light blueward of 3800 Å. Our values of  $T_{\text{eff}}$  and  $\log g$  are the same within the errors as those found by Liebert & Bergeron. Thus we adopt  $\log g = 7.38$  for the discussion below.

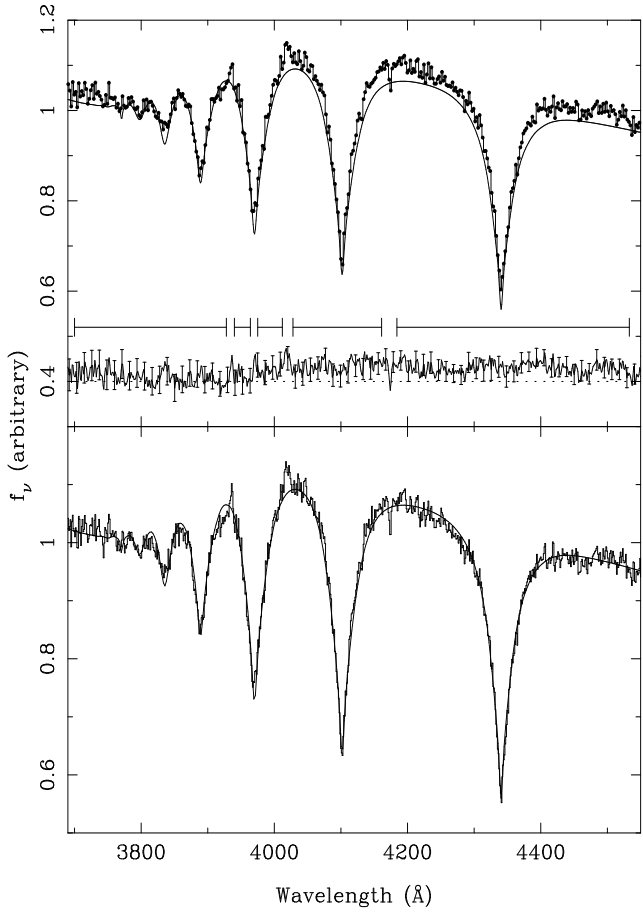


Fig. 5.— Upper panel, from top to bottom: The blue “restframe” spectrum of PG 1224+309, constructed from four spectra having a mean orbital phase of  $\phi = 0.16$  (filled circles); the best-fitting model spectrum (with  $\log g = 7.38$  and  $T_{\text{eff}} = 29,300$  K), scaled by 0.967 (smooth line); and the difference spectrum with error bars on the individual points, offset upwards by 0.4 for clarity. The horizontal bars with gaps indicate the wavelength regions used in the fit. Lower panel: The best-fitting model (smooth line) is shown with the detrended data, made by subtracting the polynomial fit to the residuals from the observed spectrum.

### 3.5. The Spectral Type of the Secondary Star

Having knowledge of the orbital ephemeris, we searched in the red spectra for the contribution of the M star and for any variations of its spectrum with orbital phase. Figure 6 shows our large-format MDM 2.4 m spectra (which cover to  $\lambda = 7500$  Å) averaged into 1/4-cycle phase bins centered on the four cardinal phases (conjunction and quadrature). Unfortunately, only a single spectrum fell in the bin nearest inferior conjunction of the M star. Nonetheless, a heating effect is clearly seen. In the lowermost spectrum (inferior conjunction), the characteristic bumpy continuum of an M dwarf is strongly present; it is less pronounced, though quite obvious, in the quadrature phases. However, in the spectrum showing the largest portion of the illuminated face (third from bottom), the M-dwarf contribution is not obvious despite good signal-to-noise. Evidently the spectrum of the illuminated face is of earlier type than the unilluminated face (or is otherwise lacking strong molecular bands), so that the bands in the observed spectrum are greatly diluted. The illumination of the M star is discussed further below.

To quantify the spectral contribution of the secondary star and estimate its type, we prepared an average of the eight large-format spectra taken within 0.2 cycle of inferior conjunction. We then systematically scaled and subtracted spectra from a library of M dwarfs. These stars were observed with the same instrumental setup, and have classifications from Boeshaar (1976). We examined the subtracted spectra looking for good cancellation of the M-dwarf features. Types M3 and earlier tended to leave a strong over-subtraction of the Na I D lines when the scale factor was set to cancel the bands in the 6500–7500 Å region, and the bands themselves did not cancel well. A spectrum of type M5 did not subtract satisfactorily. The only acceptable results were from two stars classified as M4+ (Boeshaar 1976) or M4.5 (Henry, Kirkpatrick, & Simons 1994). Figure 7 shows the best decomposition. We conclude that the intrinsic spectrum of the M dwarf is most probably a little later than M4, and that the flux contributed at this phase by the unilluminated part of the M dwarf is  $F_{\lambda} \sim 1.5 \times 10^{-16}$  erg cm $^{-2}$  s $^{-1}$  Å $^{-1}$  at 6500 Å, or 15–20 percent of the light at that wavelength. The calibration uncertainties discussed earlier should not seriously affect these conclusions, since the features cover a fairly limited wavelength range. For comparison, Orosz, Wade, & Harlow (1997) adopted a spec-

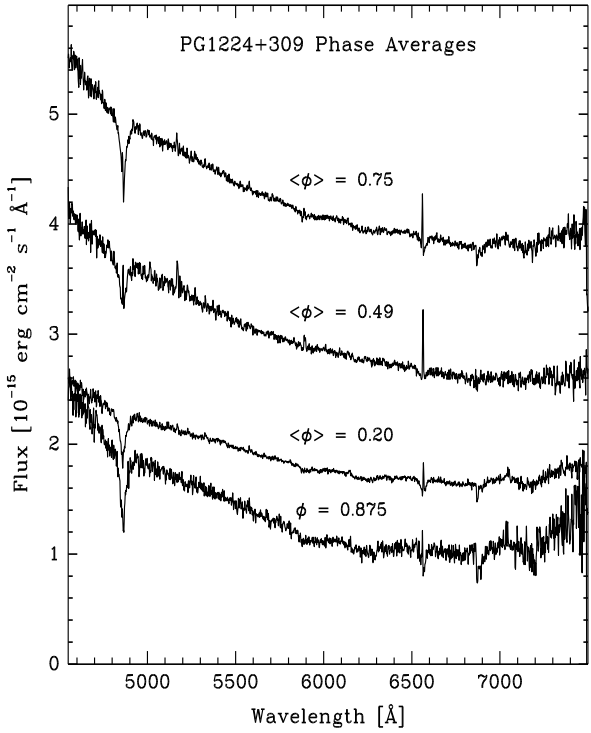


Fig. 6.— Average spectra of PG 1224+309 in 0.25-cycle phase bins. Each is labeled by its mean phase. Only one spectrum fell in the bin nearest zero phase. No scale factors are applied, and the spectra are offset from each other vertically by one unit ( $10^{-15}$  erg  $\text{cm}^{-2} \text{s}^{-1} \text{\AA}^{-1}$ ).

tral type of M1–M3 with a contribution of 10% over the region 5320–6532 Å, based on two low signal-to-noise spectra obtained near orbital phases 0.89 and 0.53.

Very few features are seen in the spectrum aside from the contributions discussed above. There is weak emission present at  $\lambda$ 5169, apparently also modulated by the illumination phase. This feature is fairly often seen in cataclysmic binaries, where it is usually attributed to Fe II (Taylor & Thorstensen 1996). Curiously, there is very little He I emission; He I is conspicuous (though weaker than the Balmer lines) in the illumination-effect stars Feige 24 (Thorstensen et al. 1978) and EUVE 2013+400 (Thorstensen et al. 1994).

Because the H $\alpha$  emission line arises mostly from one hemisphere of the M dwarf, its velocity amplitude is likely to underestimate the star's center-of-

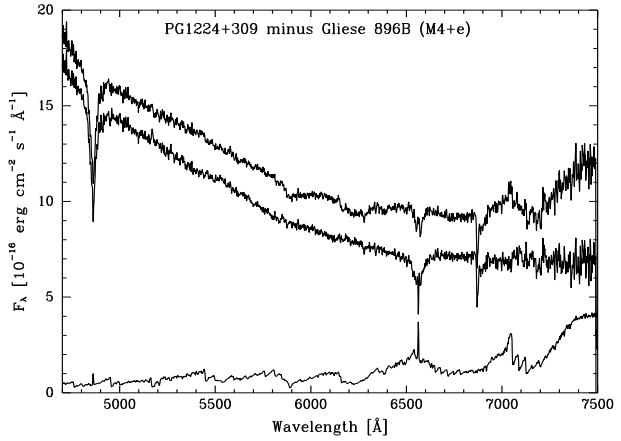


Fig. 7.— Decomposition of the spectrum. The top trace is the average of eight spectra taken within 0.2 cycles of inferior conjunction of the M dwarf. The lower trace is a scaled spectrum of Gliese 896B, spectral type M4+ (Boeshaar 1976) or M4.5V (Henry, Kirkpatrick, & Simons 1994). The middle trace is the difference of the two. The top trace is offset upward by one unit ( $10^{-15}$  erg  $\text{cm}^{-2} \text{s}^{-1} \text{\AA}^{-1}$ ) to avoid overlap with the middle trace.

mass motion. To account for this effect we tried to measure velocities of the M dwarf by cross-correlation methods, using our M dwarf library spectra (some of which have very accurate velocities from Marcy et al. 1987) as templates. Unfortunately, the signal-to-noise ratio of the available spectra proved inadequate for this purpose.

## 4. Discussion

### 4.1. Mass Constraints

Knowing the surface gravity of the white dwarf in PG 1224+309 enables us to estimate its mass. The mass–radius relation for white dwarf stars does depend on the composition of the white dwarf and its position along the cooling track. In addition, the radius will be larger for a white dwarf that has a hydrogen layer atop the degenerate core. Liebert & Bergeron (1997) estimated the mass of PG 1224+309 to be  $M_{\text{WD}} = 0.36 M_{\odot}$  based on their estimates of  $T_{\text{eff}} = 29,300$  and  $\log g = 7.38$  and using then-available evolutionary tracks for carbon-oxygen white dwarfs (cf. Wood & Winget 1989). For these same values of  $\log g$  and  $T_{\text{eff}}$ , evolutionary tracks for he-

lum white dwarfs by Althaus & Benvenuto (1997) yield  $M_{\text{WD}} = 0.40 M_{\odot}$  (their Fig. 13). These models do not include a hydrogen envelope. Benvenuto & Althaus (1998) published additional cooling tracks for helium white dwarfs that include a thin hydrogen envelope. At  $\log g = 7.38$ , these models imply  $0.40 \leq M_{\text{WD}} \leq 0.45 M_{\odot}$  for hydrogen envelope masses of  $0 \leq M_{\text{H}} \leq 4 \times 10^{-4} M_{\odot}$ . For the discussion below we will adopt  $0.35 \leq M_{\text{WD}} \leq 0.45 M_{\odot}$ .

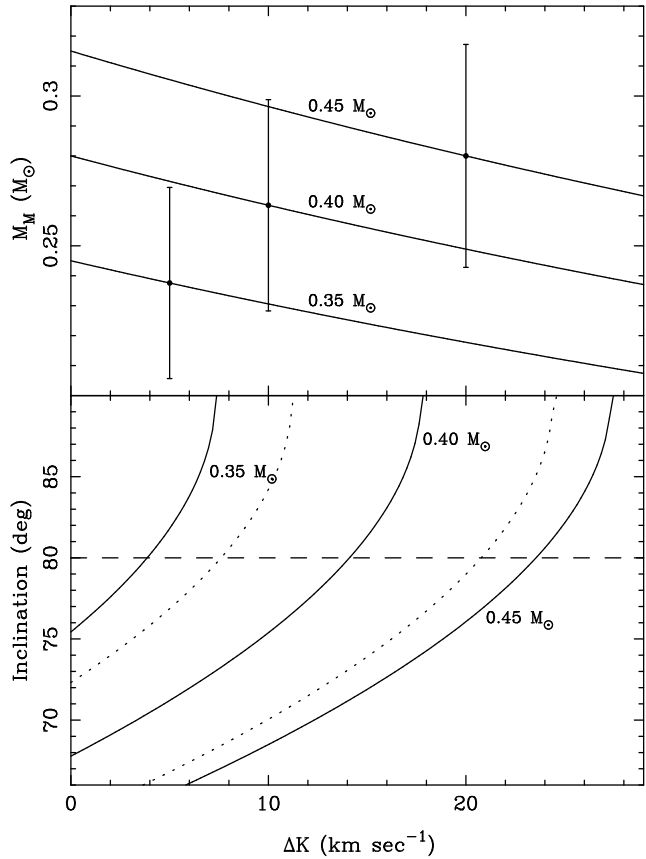


Fig. 8.— Top: The mass of the M-dwarf secondary as a function of  $\Delta K$  for  $M_{\text{WD}} = 0.35 M_{\odot}$ ,  $M_{\text{WD}} = 0.40 M_{\odot}$ , and  $M_{\text{WD}} = 0.45 M_{\odot}$ , assuming  $K_{\text{WD}} = 112 \pm 14 \text{ km s}^{-1}$  and  $K_{\text{H}\alpha} = 160 \pm 8 \text{ km s}^{-1}$ . The sizes of the statistical errors on  $M_{\text{M}}$  are illustrated by the three points with error bars. Bottom: The derived inclination as a function of  $\Delta K$  for  $M_{\text{WD}} = 0.35 M_{\odot}$ , and  $M_{\text{WD}} = 0.40 M_{\odot}$ ,  $M_{\text{WD}} = 0.45 M_{\odot}$ . The dashed lines indicate the range of allowed solutions for the  $M_{\text{WD}} = 0.40 M_{\odot}$  case, propagating one-sigma errors in  $K_{\text{WD}}$  and  $K_{\text{H}\alpha}$ .

The measured orbital velocities of the two stars determine the mass ratio:  $Q = M_{\text{M}}/M_{\text{WD}} = K_{\text{WD}}/K_{\text{M}}$ . If  $Q$  were known accurately, then  $M_{\text{M}}$  and the total mass of PG 1224+309 would simply scale from  $M_{\text{WD}}$  as estimated above. The velocity semiamplitude of the white dwarf was measured reliably from the higher Balmer lines visible in the Lick spectra:  $K_{\text{WD}} = 112 \pm 14 \text{ km s}^{-1}$ . On the other hand, the M star's orbital speed is not directly measured, since the center of light of the  $\text{H}\alpha$  line emission does not correspond to the center of mass of the M star,  $K_{\text{M}} = K_{\text{H}\alpha} + \Delta K$ . Since the  $\text{H}\alpha$  emission line is formed in the heated face of the M star, we expect  $\Delta K > 0$ , or  $Q = K_{\text{WD}}/(K_{\text{H}\alpha} + \Delta K) < 0.700 \pm 0.094$ , using the adopted  $K_{\text{H}\alpha} = 160 \pm 8 \text{ km s}^{-1}$ .

We can express  $\Delta K$  as

$$\Delta K = \frac{\Delta R}{a} (1 + Q) K_{\text{M}}$$

where  $\Delta R$  is the shift of the “effective center” of the  $\text{H}\alpha$  emission line with respect to the center of mass of the M star (Wade & Horne 1988) and the orbital separation is  $a = 1.71(M_{\text{total}}/M_{\odot})^{1/3} R_{\odot}$ . In the case of a synchronously rotating M star with uniform  $\text{H}\alpha$  emission over one hemisphere and no  $\text{H}\alpha$  emission over the other,  $\Delta R = 4R_{\text{M}}/(3\pi)$ , where  $R_{\text{M}}$  is the radius of the M star. To complete an estimate of  $\Delta K$ , we temporarily adopt values for  $R_{\text{M}}$  of  $0.25 \pm 0.01 R_{\odot}$  and for  $M_{\text{M}}$  of  $0.25 \pm 0.01 M_{\odot}$ , based on the dM4e eclipsing binary CM Draconis (Lacy 1977). Using  $M_{\text{WD}} = 0.4 \pm 0.05 M_{\odot}$ , we then find  $Q = 0.625$  and  $M_{\text{total}} = 0.65 M_{\odot}$ . Using  $K_{\text{H}\alpha} = 160 \pm 8 \text{ km s}^{-1}$ , we find  $\Delta K = 21 \pm 2 \text{ km s}^{-1}$ .

The true value of  $\Delta K$  probably cannot be lower than our rough estimate of  $21 \text{ km s}^{-1}$ , since  $\Delta R$  will be larger if the  $\text{H}\alpha$  emission is more concentrated to the regions of the M star closest to the white dwarf (we argued above in Section 3.1 that the M star probably has very little intrinsic  $\text{H}\alpha$  emission). In principle,  $\Delta R$  could be as large as  $R_{\text{M}}$  ( $\Delta K = 49 \text{ km s}^{-1}$ ), but then one would not expect to see the equivalent width of  $\text{H}\alpha$  varying sinusoidally, as actually observed. Tighter upper limits on  $Q$  and  $\Delta K$  come from considering the orbital inclination, which must be less than about  $80^\circ$  since there are no eclipses longer than about 0.03 in phase. (Light curve modeling is discussed further below.)

For an assumed value of  $\Delta K$ , the measured values of  $P$ ,  $K_{\text{WD}}$  and  $K_{\text{H}\alpha}$ , and our estimate of  $M_{\text{WD}}$  from  $\log g$ , we compute  $Q$  and  $M_{\text{total}}$ , and we infer

the orbital inclination  $i$ . This is shown in the lower panel of Figure 8 for  $M_{\text{WD}} = 0.35 M_{\odot}$ ,  $0.40 M_{\odot}$ , and  $0.45 M_{\odot}$ . The upper panel of Figure 8 shows  $M_{\text{M}}$  vs.  $\Delta K$ . If  $M_{\text{WD}} = 0.35 M_{\odot}$ ,  $\Delta K$  must be less than  $\approx 7.2 \text{ km s}^{-1}$  to allow  $i \leq 90^\circ$ , and if  $i < 80^\circ$  as suggested by the absence of eclipses,  $\Delta K \lesssim 4 \text{ km s}^{-1}$ , much less than our estimate of  $\Delta K \approx 21 \text{ km s}^{-1}$ . For  $M_{\text{WD}} = 0.4 M_{\odot}$  and  $i < 80^\circ$ , allowed values of  $\Delta K$  ( $\lesssim 14 \text{ km s}^{-1}$ ) are still smaller than  $21 \text{ km s}^{-1}$ . In order to have  $\Delta K \gtrsim 21 \text{ km s}^{-1}$ ,  $M_{\text{WD}} \gtrsim 0.45 M_{\odot}$  is required. Taken at face value, this “large” white dwarf mass favors the white dwarf models with a “thick” hydrogen envelope ( $M_{\text{H}} = 4 \times 10^{-4} M_{\odot}$ , Benvenuto & Althaus 1998).

For  $\Delta K = 21 \pm 2 \text{ km s}^{-1}$  and  $M_{\text{WD}} = 0.45 \pm 0.05 M_{\odot}$ , the mass of the M star is  $M_{\text{M}} = 0.28 \pm 0.05 M_{\odot}$ ,  $i = 77 \pm 7^\circ$ , and  $Q = 0.62 \pm 0.08$ , where we have propagated the errors on  $K_{\text{WD}}$  and  $K_{\text{H}\alpha}$ . The mass of the M star is not too different from the measured masses of the dM4e components of CM Draconis:  $M = 0.237$  and  $0.207 M_{\odot}$ , with errors of 4% (Lacy 1977). When  $M_{\text{WD}} = 0.45 M_{\odot}$ , increasing  $\Delta K$  by  $5 \text{ km s}^{-1}$  reduces  $M_{\text{M}}$  by  $0.015 M_{\odot}$ .

To summarize the argument: so far we have discussed a mass estimate for the secondary star based on orbital dynamics. The two uncertain quantities in the analysis are  $M_{\text{WD}}$ , made uncertain by the unknown H envelope mass, and  $\Delta K$ . Adopting a plausible value for  $\Delta K$  (based partly on the radii of the components of CM Dra, which has a similar spectral type) leads to an estimate of  $M_{\text{M}}$  that is consistent with the more massive component of CM Dra. This is consistent, if slightly circular reasoning, but it suggests that the inclination of the binary orbit plane is fairly high. To avoid eclipses, however,  $i$  must not be too high, and thus higher stellar masses are favored, in order to account for the observed radial velocity amplitudes.

An alternate method of estimating the mass uses an empirical mass-luminosity relation for M dwarfs, as follows. From the white dwarf’s  $T_{\text{eff}}$  and  $\log g$  and assuming  $M_{\text{H}} = 0$  ( $M_{\text{WD}} = 0.40 M_{\odot}$ ) we find  $\log L_{\text{WD}}/L_{\odot} = -0.5$  (Althaus & Benvenuto 1997), and thus  $M_{\text{bol}}(\text{WD}) = 6.00$ . Using computed bolometric corrections and colors for hydrogen atmosphere white dwarfs from Bergeron et al. (1995; for  $T_{\text{eff}} = 30,000 \text{ K}$  and  $\log g = 8$ ), we then find  $M_V(\text{WD}) = 8.966$  and  $M_R(\text{WD}) = 9.095$ . From the spectral decomposition described above, the M star contributes  $\approx 16\%$  of the light in  $R$ , so  $M_R(\text{M}) =$

10.90. According to Kirkpatrick & McCarthy (1994), an M4.5V star has  $V - R = 1.37$ , so  $M_V(\text{M}) = 12.27$ . Finally, Henry & McCarthy (1993) give the relation  $\log M_{\text{M}}/M_{\odot} = -0.1681M_V + 1.4217$  with an rms scatter in  $\log M/M_{\odot}$  of 0.081. From this,  $M_{\text{M}} = 0.23 \pm 0.04 M_{\odot}$ . The M star’s mass inferred by this method is slightly higher (by  $\approx 0.02 M_{\odot}$ ) if the white dwarf’s hydrogen layer mass is  $M_{\text{H}} = 4 \times 10^{-4} M_{\odot}$ , because the higher white dwarf mass ( $0.45 M_{\odot}$ , Benvenuto & Althaus 1998) implies a slightly larger radius for the white dwarf (at fixed gravity), hence higher luminosities for both stars. Either value of  $M_{\text{M}}$  is consistent with the orbit-based mass estimate.

As an aside, we can compute the distance to the system. The  $R$  magnitude of the system at phase 0.0 (when the contribution of the heated face of the M star is minimal) is  $R = 16.22$ . The white dwarf contributes 84% of the light in  $R$ , hence the apparent  $R$  magnitude of the white dwarf by itself is  $m_R(\text{WD}) = 16.22 - 2.5 \log 0.84 = 16.41$ . The distance is then  $d = 290 \text{ pc}$  ( $0.4 M_{\odot}$  white dwarf) or  $d = 308 \text{ pc}$  ( $0.45 M_{\odot}$  white dwarf).

## 4.2. Light Curve Models

The light curves described above show no obvious eclipses and are nearly sinusoidal. They are thus consistent with a very simple picture of the light modulation in PG 1224+309 being due to phase-dependent visibility of the bright, inward-facing hemisphere of a nearly spherical secondary star, which is uniformly emitting as a consequence of strong heating by the white dwarf. If one were sure of the radiative properties of both illuminated and unilluminated sides of the M dwarf (i.e., if one knew the surface fluxes and limb-darkening coefficients in each color), one could model the light curves to infer constraints on the radius of the M dwarf and on the inclination. Such radiative quantities are becoming available for normal, unilluminated photospheres of low-luminosity stars (cf. Claret 1998 for limb-darkening coefficients based on the Next-Gen model atmospheres of Hauschildt et al. 1998). For the strongly illuminated hemisphere, however, neither surface fluxes nor limb-darkening behavior is known. Treating the problem by assuming that the atmosphere behaves “normally,” i.e. with standard albedo and limb-darkening coefficients at an enhanced effective temperature, is not adequate for making robust conclusions regarding the secondary star (cf. Hilditch et al. 1996, who review problems of light-curve synthesis for strongly irradiated stars, in-

cluding the formal finding of limb-*brightening* in their analysis of the systems AA Dor and KV Vel).

In view of this difficulty, we are content here to check whether the light curve amplitudes can be approximately reproduced, using properties of the stars and the binary orbit consistent with our prior discussion, and without requiring such an extreme inclination as to introduce an eclipse or other large distortion. Essentially, the question reduces to whether the pair of quantities  $i$  and  $R_M/a$  that is needed to model the light curves is consistent with the properties of PG 1224+309 as known from the discussion given above. For this purpose, a simplified treatment using black-body emissivities (at the local effective temperature) and a limb-darkening law appropriate for (unilluminated) cool photospheres *may* be adequate.

We used the Wilson–Devinney (W–D; 1971) light curve synthesis code, fixing the temperature of the white dwarf at 29,300 K. The M star’s temperature was fixed at 3100 K (unilluminated). The gravity darkening coefficients for the two stars were 1.0 and 0.3, respectively. The bolometric albedos for reflection heating and re-radiation were set to 1.0 and 0.5, respectively. For definiteness, a limb-darkening law was used that includes a logarithmic term and took the appropriate coefficients for the four filters from the tables in Van Hamme (1993). In the W–D code, the fractional radii  $R/a$  are expressed in terms of the mass ratio and the so-called  $\Omega$ -potentials of the two stars. The inclination and mass ratio were varied on a grid,  $70^\circ \leq i \leq 79^\circ$  and  $0.52 \leq Q \leq 0.71$ . For  $i > 79^\circ$  eclipses are predicted. At each grid point, and assuming values for the  $\Omega$ -potentials, the  $B$ ,  $V$ ,  $R$ , and  $I$  light curves were fitted simultaneously, and the values of  $\Omega_{WD}$  and  $\Omega_M$  were adjusted to find the minimum  $\chi^2$ . In general, the best-fitting models underestimated the amplitude of the  $B$  light curve, matched more or less the amplitudes of the  $V$  and  $R$  light curves, and overestimated the amplitude of the  $I$  light curve. In view of the modeling uncertainties in the case of strongly illuminated stars, the ability of the W–D code to roughly match the observed light-curve amplitudes for plausible values of  $i$ ,  $Q$  and  $\Omega_M$  is regarded as confirmation of the basic picture we have of PG 1224+309.

### 4.3. Prospects for Improved Understanding of PG 1224+309

Without the benefit of eclipses, how can accurate masses of the component stars of PG 1224+309 be

derived? Additional observables include the M star’s rotational velocity  $v_{\text{rot}} \sin i$  and a direct measurement of  $K_M$  from absorption lines. The rotational velocity could be exploited, assuming synchronous rotation, to form the ratio  $R_M/a_M$  where  $a_M$  is the size of the M star’s orbit around the center of mass. An absorption line velocity curve, depending on the lines used, would give an estimate of  $K_M$  requiring a “K-correction” of the opposite sign to that used here.

Additional information could be extracted from the light curves, given improved theoretical modeling of irradiated atmospheres, to be incorporated into light-curve synthesis codes. In particular, believable light-curve amplitudes could be used to specify the radius of the M star, relative to the orbital separation, as a function of the orbital inclination. Consistency between inferred mass and radius could then be demanded, to sharply limit the allowed range of inclination.

In principle, one could measure the gravitational redshift of the white dwarf which would provide an independent constraint on the mass and radius of the white dwarf. The gravitational redshift would simply be the difference in the two  $\gamma$  values for the orbital solutions of the two components. Currently, the measured  $\gamma$  values are not known well enough, both in terms of formal statistical errors and in terms of systematic errors, to enable a meaningful measurement of the gravitational redshift ( $\gamma_{WD} = -4 \pm 12 \text{ km s}^{-1}$  and  $\gamma_{H\alpha} = 10 \pm 6 \text{ km s}^{-1}$ ; statistical errors are quoted). The Balmer lines have sharp emission features in their cores, which complicates the measurement of  $\gamma_{WD}$ . Possibly the white dwarf has metal absorption lines in the ultraviolet, in which case a spaced-based measurement of  $\gamma_{WD}$  might be possible.

Finally, some improvement in the measurement of  $K_{WD}$  might be achieved from additional spectroscopy covering the entire orbital cycle.

### 4.4. Evolutionary Considerations

#### 4.4.1. The Past: PG 1224+309 as a Post-Common Envelope Binary

The present orbital separation of PG 1224+309 is  $a \approx 1.5 R_\odot$ . The present white dwarf was once the core of a giant star with a radius of  $\approx 100 R_\odot$  and therefore  $a > 100 R_\odot$  formerly. The standard picture of how such initially wide binaries can be drastically reduced in orbital size is the so-called “common envelope” (CE) process. Very roughly, in this picture the

envelope of the growing giant star engulfs the companion star, and orbital energy is lost due to friction against the envelope, leading to the possible ejection of the envelope. Iben & Livio (1993) present a well-organized and relatively recent review of the CE process and the stellar evolution scenarios and products involving it. Livio (1996) reviews how observations can further constrain the CE scenarios.

The CE phase is very short-lived, and it unlikely to be observed directly, but post-CE binaries such as PG 1224+309 have the potential to illuminate some aspects of the CE process. One question of interest is whether a rule can be given for terminating the decay of the binary orbit — does the decay continue until essentially all material outside the (pre-white dwarf) “core” of the giant star has been expelled, and if so what is the mass of the residual hydrogen envelope? In PG 1224+309,  $M_{\text{WD}}$  as inferred from  $T_{\text{eff}}$  and  $\log g$  is ambiguous at the 0.05  $M_{\odot}$  level, unless the hydrogen envelope mass  $M_{\text{H}}$  is known. Given an estimate of  $M_{\text{WD}}$ , however, we can infer  $M_{\text{M}}$  along with the orbital inclination, from  $\Delta K$  and the mass ratio. With our best estimate of  $\Delta K$ , the lack of eclipses favors a higher white dwarf mass, hence a relatively thick hydrogen envelope. PG 1224+309 misses being an eclipsing system by only a few degrees! Eclipses would provide additional constraints on the mass and radius of the white dwarf. It would then be possible to infer  $M_{\text{H}}$  with high confidence. This would be a new and valuable piece of information with which to confront common-envelope theories.

Systems like PG 1224+309 can also sometimes be used to study the efficiency of the common envelope process. This is usually parameterized by the parameter  $\alpha_{\text{CE}}$ , which relates the initial and final orbits to the energy expended in ejecting the CE. The efficiency thus helps to determine the mapping of initial binary periods onto final (post-CE) periods. Except for the ambiguity in  $M_{\text{WD}}$ , PG1224+309 would be a useful system in potentially giving a lower limit to  $\alpha_{\text{CE}}$ . The argument is as follows. The decay of the orbit must have released enough energy to overcome the binding energy of the envelope that formerly blanketed the white dwarf. The supply of orbital energy can be estimated from the present separation and masses (there is little dependence on the initial separation), and the present mass of the white dwarf gives the radius of its giant star progenitor at the moment that dynamical timescale mass transfer began (*via* the giant branch core-mass – luminosity relation). That radius, com-

bined with an estimate of the envelope mass, gives the binding energy of the envelope. The ratio defines  $\alpha_{\text{CE}}$ :  $E_{\text{bind}} = \alpha_{\text{CE}} \Delta E_{\text{orbit}}$  or

$$\frac{M_1(M_1 - M_{1R})}{\lambda a_o r_L} = \alpha_{\text{CE}} \left( \frac{M_{1R}M_2}{2a_f} - \frac{M_1M_2}{2a_o} \right)$$

using the definitions of Webbink (1984) as given in Livio (1996). Here  $M_1$  and  $M_2$  are the initial masses,  $M_{1R}$  is the core or remnant mass of the more evolved star,  $a_o$  and  $a_f$  are the original and final orbital separations,  $r_L$  is the radius of the evolved star’s original Roche lobe expressed as a fraction of  $a_o$ , and  $\lambda = 0.5$  is a structure factor for that star’s envelope.

The calculated value of  $\alpha_{\text{CE}}$  depends strongly on the assumed core mass  $M_{1R} = M_{\text{WD}}$ . For PG 1224+309, we first consider the case where  $M_{1R} = M_{\text{WD}} = 0.40 M_{\odot}$ ,  $M_2 = 0.25 M_{\odot}$ , and  $a_f = 1.48 R_{\odot}$ . Then the available orbital energy was about  $\Delta E_{\text{orbit}} = 3.4 \times 10^{-2}$  in solar units with  $G = 1$ . Here we neglect the small second term on the R.H.S. of the displayed equation. For assumed initial masses of  $M_1 = 1.0$ ,  $1.2$ , and  $1.4 M_{\odot}$ , the radius of the star when it contacted its Roche lobe and began mass transfer leading to the common envelope was  $R_{\text{lobe}} = a_o r_L = 75$ ,  $71$ , or  $68 R_{\odot}$  (using approximations from Tout et al. 1997). The binding energy of the envelope was approximately  $E_{\text{bind}} = 1.6 \times 10^{-2}$ ,  $2.7 \times 10^{-2}$ , and  $4.1 \times 10^{-2}$ , respectively. With these assumptions, the available orbital energy exceeded the binding energy only if  $M_1$  was less than  $1.4 M_{\odot}$ , and even then most of the orbital energy was needed to unbind the envelope; thus  $\alpha_{\text{CE}}$  cannot have been significantly less than unity. (Stars with values of  $M_1$  much smaller than those considered are less likely to have evolved so far yet. Also, for  $M_{1R} = 0.4 M_{\odot}$ , which corresponds to a luminosity well below the tip of the red giant branch, mass loss on the giant branch is not likely to have been significant.) By this example we have shown how, in principle, observations of relatively wide post-CE binaries (with small negative orbital energies) set a lower limit on  $\alpha_{\text{CE}}$ . However, in the specific case of PG 1224+309, the ambiguity in  $M_{\text{WD}}$  owing to our ignorance of  $M_{\text{H}}$  makes this particular test less interesting. This is because increasing  $M_{\text{WD}}$  to  $\approx 0.45 M_{\odot}$  reduces the pre-CE binding energy greatly and thus reduces the lower limit on  $\alpha_{\text{CE}}$ . Finding *eclipsing*, double-lined DA+dM systems may in favorable cases provide firmer constraints on  $\alpha_{\text{CE}}$ . Analogous eclipsing systems would allow better constraints to be placed on the component masses and

radii, which would in turn allow one to begin addressing additional questions, such as whether post-CE secondaries satisfy a normal main sequence mass-radius relation.

#### 4.4.2. The Future: PG 1224+309 as a Pre-Cataclysmic Binary

PG 1224+309 is a post-CE binary, as discussed above, and is also a pre-cataclysmic binary in the sense of Ritter (1986): the orbital separation  $a$  will shrink owing to gravitation wave radiation (GWR) until the M star contacts its Roche lobe and initiates mass transfer onto the white dwarf. (Angular momentum loss *via* magnetic braking, another process considered by Ritter, is thought not to operate for low-mass M dwarfs.) Using formulae from Ritter (1986) and adopting  $M_{\text{WD}} = 0.45 M_{\odot}$  and  $M_{\text{M}} = 0.28 M_{\odot}$ , it will take about  $9.0 \times 10^9$  years for GWR to bring PG 1224+309 into a semidetached configuration, at which time the orbital period will be 2.5 hours. The present cooling age of the white dwarf is perhaps a few  $\times 10^7$  years (Althaus & Benvenuto 1997), but when Roche-lobe overflow (RLOF) mass transfer begins the white dwarf will have cooled to well below  $T_{\text{eff}} = 5000$  K.

## 5. Summary

We have measured the orbital period of PG 1224+309 to be  $P = 0.258689 \pm 0.000004$  days. The semi-amplitude of the white dwarf's radial velocity curve is  $K_{\text{WD}} = 112 \pm 14$  km s $^{-1}$ . The velocity semi-amplitude of the H $\alpha$  emission line arising from the irradiated hemisphere of the M star is  $K_{\text{H}\alpha} = 160 \pm 8$  km s $^{-1}$ . We estimate a "K-correction" of  $\Delta K = 21 \pm 2$  km s $^{-1}$ , where  $K_{\text{M}} = K_{\text{H}\alpha} + \Delta K$ . The implied mass ratio is then  $Q = M_{\text{M}}/M_{\text{WD}} = 0.62 \pm 0.08$ . The spectral type of the secondary is M4+. We fit synthetic spectra to the blue spectrum and find  $T_{\text{eff}} = 29,300$  K and  $\log g = 7.38$  for the white dwarf. The white dwarf contributes 97% of the light at 4500 Å and virtually all of the light blueward of 3800 Å.

The mass inferred for the white dwarf depends on the assumed mass of the thin residual hydrogen envelope:  $0.40 \leq M_{\text{WD}} \leq 0.45 M_{\odot}$  for hydrogen envelope masses in the range  $0 \leq M_{\text{H}} \leq 4 \times 10^{-4} M_{\odot}$ . Given the absence of eclipses, for likely values of  $\Delta K$  and based on the observed values of  $K_{\text{WD}}$  and  $K_{\text{M}}$ , we conclude that the mass of the white dwarf is closer to  $0.45 M_{\odot}$ . It thus appears that the white dwarf has a

relatively large residual hydrogen envelope. The mass of the M star is  $M_{\text{M}} = 0.28 \pm 0.05 M_{\odot}$  if  $\Delta K = 21 \pm 2$  km s $^{-1}$  and  $M_{\text{WD}} = 0.45 \pm 0.05 M_{\odot}$ . In this case, the inclination is  $i = 77 \pm 7^\circ$ , only a few degrees away from giving rise to eclipses. Additional observational and theoretical work could improve our knowledge of the masses of the component stars.

We argued that an accurately determined residual hydrogen envelope mass can constrain theories of common envelope evolution, and we showed how accurate values of  $M_{\text{WD}}$  in binaries such as PG 1224+309 can help set limits on  $\alpha_{\text{CE}}$ , the efficiency parameter used in common envelope scenarios. PG 1224+309 itself will become a cataclysmic variable with an orbital period of about 2.5 hours, after a further  $\approx 10^{10}$  years of orbital evolution.

This work was partially supported by a grant from NASA administered by the American Astronomical Society. JRT and CJT thank the NSF for support through grant AST-9314787, and the MDM staff for their usual excellent support. M. E. acknowledges support from Hubble fellowship grant HF-01068.01-94A from Space Telescope Science Institute, which is operated for NASA by the Association of Universities for Research in Astronomy, Inc., under contract NAS 5-26255. We thank Ivan Hubeny for instruction in the use of his stellar atmosphere codes TLUSTY, SYNSPEC, and ROTINS.

## REFERENCES

- Althaus, L. G., & Benvenuto, O. G. 1997, ApJ, 477, 313
- Benvenuto, O. G., & Althaus, L. G. 1998, MNRAS, 293, 177
- Bergeron, P., Wesemael, F., & Beauchamp, A. 1995, PASP, 107, 1047
- Boeshaar, P. 1976, Ph. D. Thesis, Ohio State University
- Chavira, E. 1958, Bol. Obs. Tonantzintla y Tacubaya, 2 (No. 18), 3
- Claret, A. 1998, A&A, 335, 647
- Ferguson, D. H., Green, R. F., & Liebert, J. 1984, ApJ, 287, 320
- Green, R. F., Schmidt, M., & Liebert, J. 1986, ApJS, 61, 305

Hauschildt, P. H., Allard, F., & Baron, E. 1988, *ApJ*, in press (astro-ph 9807286)

Henry, T. J., & McCarthy, Jr., D. W. 1993, *AJ*, 106, 773

Henry, T. J., Kirkpatrick, J. D., & Simons, D. A. 1994, *AJ*, 108, 1437

Hilditch, R. W., Harries, T. J., & Hill, G. 1996, *MNRAS*, 279, 1380

Hubeny, I., & Lanz, T. 1997, “SYNSPEC — A User’s Guide, Version 42”

Iben, Jr., I., & Livio, M. 1993, *PASP*, 105, 1373

Iriarte, B., & Chavira, E. 1957, *Bol. Obs. Tonantzintla y Tacubaya*, 3 (No. 22), 37

Kirkpatrick, J. D., & McCarthy, Jr., D. W. 1994, *AJ*, 107, 333

Lacy, C. H., 1977, *ApJ*, 218, 444

Landolt, A. U. 1992, *AJ*, 104, 340

Liebert, J. W., & Bergeron, P. 1997, private communication

Livio, M. 1996, in *Origins, Evolutions, and Destinies of Binary Stars in Clusters*, eds. E. F. Milone & J.-C. Mermilliod, *ASP Conf. Ser.* 90, 291

Marcy, G. W., Lindsay, V., & Wilson, K. 1987, *PASP*, 99, 490

Marsh, T. R., Robinson, E. L., & Wood, J. H. 1994, *MNRAS*, 266, 137

Miller, J. S., & Stone, R. P. S. 1993, *Lick Obs. Tech. Rep.*, No. 66

Orosz, J. A., Wade, R. A., & Harlow, J. J. B. 1997, *AJ*, 114, 317

Ritter, H. 1986, *A&A*, 169, 139

Sanduleak, N., & Pesch, P. 1984, *ApJS*, 55, 517

Schneider, D. and Young, P. 1980, *ApJ*, 238, 946

Stetson, P. B. 1987, *PASP*, 99, 191

Stetson, P. B., Davis, L. E., & Crabtree, D. R. 1991, in “CCDs in Astronomy,” ed. G. Jacoby, *ASP Conference Series*, Volume 8, page 282

Stetson, P. B. 1992a, in “Astronomical Data Analysis Software and Systems I,” eds. D. M. Worrall, C. Biemesderfer, & J. Barnes, *ASP Conference Series*, Volume 25, page 297

Stetson, P. B. 1992b, in “Stellar Photometry—Current Techniques and Future Developments,” *IAU Coll.* 136, eds. C. J. Butler, & I. Elliot, Cambridge University Press, Cambridge, England, page 291

Taylor, C. J., & Thorstensen, J. R. 1996, *PASP*, 108, 894

Thorstensen, J. R., Charles, P. A., Margon, B., & Bowyer, S. 1978, *ApJ*, 223, 260

Thorstensen, J. R., Patterson, J., Shambrook, A., and Thomas, G. 1996, *PASP* 108, 73

Thorstensen, J. R., Vennes, S. & Shambrook, A. 1994, *AJ*, 108, 1924

Tout, C. A., Aarseth, S. J., Pols, O. R. & Eggleton, P. P. 1997, *MNRAS*, 291, 732

Van Hamme, W. 1993, *AJ*, 106, 2096

Vennes, S., & Thorstensen, J. R. 1994, *ApJ*, 433, L29

Wade, R. A., & Horne, K. 1988, *ApJ*, 324, 411

Webbink, R. F. 1984, *ApJ*, 277, 355

Wilson, R. E., & Devinney, E. J. 1971, *ApJ*, 166, 605

Wood, M. A., & Winget, D. E. 1989, in “White Dwarfs,” ed. G. Wegner, Springer-Verlag, Berlin, page 282